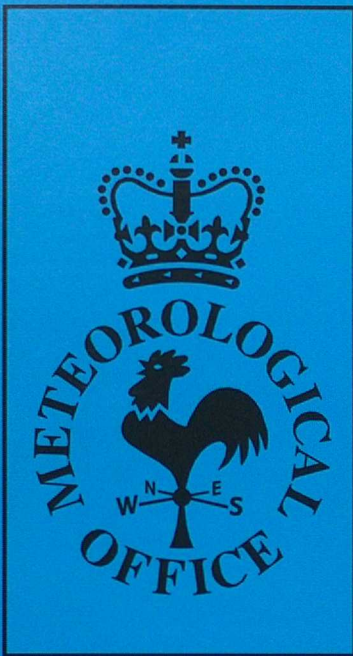


DUPLICATE



Forecasting Research

Forecasting Research Division
Technical Report No. 161

Enhancement of the Nimrod Satellite Precipitation
Scheme to diagnose Rainfall Rate

by

R Brown

25 April 1995

Meteorological Office
London Road
Bracknell
Berkshire
RG12 2SZ
United Kingdom

ORGS UKMO F

National Meteorological Library
FitzRoy Road, Exeter, Devon. EX1 3PB

Forecasting Research Division

Technical Report No.161

Enhancement of the Nimrod Satellite Precipitation Scheme
to diagnose Rainfall Rate

by

R Brown

25 April 1995

© Crown Copyright 1995

Forecasting Research
Meteorological Office
London Road
Bracknell
Berkshire RG12 2SZ
ENGLAND

N.B This paper has not been published. Permission to quote from it must be obtained from the above Met. Office branch.

Enhancement of the Nimrod Satellite Precipitation Scheme to diagnose Rainfall Rate

R Brown, FR Division

25 April 1995

1. Introduction

The Nimrod satellite precipitation scheme has been enhanced to diagnosed areas with rainfall rates in excess of three thresholds, besides rain/no rain. The thresholds used are 0.125, 0.5 and 2 mmh⁻¹. The satellite precipitation field containing rainfall rate information is to be used in the Nimrod overall rainfall analysis.

The method used is described in this note. Since this is basically the same as used for rain/no rain discrimination, "universal tables" are also required for each threshold and their derivation is also described. Finally, some statistics are presented on the performance of the correlation technique for each threshold.

2. Methodology

The current method used to diagnose rain above a threshold of 0.03 mmh⁻¹ (ie rain/no rain) is described first, since this applies to all thresholds. It is based on the correlation technique of Lovejoy and Austin (1979). The satellite data is first reduced to 32 classes for use in the 1-D tables (ie visible or infrared data alone) or 16 classes for use in the 2-D tables. The radar data is reduced to rain (= 1) and no rain (= 0). Within the radar area, defined by the FRONTIERS shallow layer Usable Data Boundary (UDB) during the tests and the Area of Rainfall Coverage (ARC) in Nimrod, the radar and satellite data are compared pixel by pixel in order to build up tables of rain and no rain counts in each satellite class. Thus 6 tables are produced, based on visible data alone, infrared data alone and both together in a 2-D table. These tables, containing only satellite data at the current time, are known as current tables. Six time-averaged tables are also produced and these are known as recent tables. The recent tables are updated with each new set of satellite data according to :-

$$\text{Recent Counts}_t = 0.7 \times \text{Recent Counts}_{t-1} + 0.3 \times \text{Current Counts}$$

for each satellite class.

From the rain and no rain count tables, tables of the percentage of rain in each class are produced. The satellite classes are then assigned as rain, starting with the class exhibiting the highest percentage of rain counts and then working down the classes in order of percentage of rain. After each class is assigned, the total number of satellite-diagnosed rain pixels is compared with the total observed by radar. The assignation stops with the class which produces the closest match to the radar total. This is known as the critical class and the percentage of rain counts in this class is the critical percentage. Note that the classes assigned as rain need not be contiguous.

When visible and infrared data are available, three satellite precipitation fields are produced. Each pixel is assigned first using the current table. Satellite classes not assigned in the current tables (because there were too few counts in the radar area) are assigned using the recent tables and those not in the recent tables assigned using the universal tables. If both satellite fields are present then it is necessary to choose the best field from visible, infrared and 2-D. This is done by comparing each with the radar field within the radar area. The precipitation field producing the highest tetrachoric correlation coefficient is selected.

The software has been converted to diagnose areas where the rainfall rate is above any of the thresholds by adding an extra DO loop after slicing the satellite data. The radar data is then sliced into 0 (rain rate below the threshold) or 1 (rain rate equal to or above the threshold) each time around the loop. The computation then proceeds as described above. The current tables and main arrays are therefore reused each time around the rainfall rate loop. However, different recent and universal tables have to be used for each threshold. The development of the universal tables is described in the next section.

At the end of each pass through the rainfall rate loop, if visible and infrared data are available, three satellite precipitation fields are produced and compared with the sliced radar data. The best is used to construct the final satellite precipitation field. This is assigned as for the rain/no rain case, except a pixel can only be assigned as being above a threshold if it has already been assigned as being above all lower thresholds. It is hoped that this will provide some quality control on the diagnosis of the higher thresholds. The final satellite precipitation field contains zeroes for no rain, 1 for >0.03 , 2 for >0.125 , 3 for >0.5 and 4 for >2 mmh^{-1} . It should be noted that the program logic, which was adopted to minimize alterations to the original software, means that the satellite precipitation field between 0.03 and 0.125 mmh^{-1} could be assigned from visible alone say and the part between 0.125 and 0.5 mmh^{-1} from the 2-D tables and so on. During the tests this did not appear to happen, the same method being best for all thresholds.

3. Generation of Universal Tables for the Non-zero Rainfall Rates

The original universal tables comprise a threshold in the case of 1-D tables and a boundary in the 2-D tables, which separate rain and no rain satellite classes. It has been necessary to generate these for the rainfall rate thresholds, where of course they separate satellite classes associated with rates above and below the threshold rate. The thresholds and boundaries were produced from aggregate tables of rain and no rain counts as had been done previously by Cheng et al. (1993). A version of the satellite software was produced (SATAGG.FOR) which produced aggregate tables in place of the recent tables in subroutine CORTAB. All subroutines after CORTAB were deleted, since the only output required from SATAGG was the aggregate tables.

An array of radar rainfall rates was also passed to CORTAB and used to produce aggregate rainfall rates and aggregate rainfall rate squared. These were used to produce the mean and standard deviation of the rainfall rate in each satellite class. These were not required to produce the universal tables but were produced to give more insight into the ability of the satellite data to delineate rainfall rates.

Aggregate tables were produced using data from 7 days: 13 Nov. 91 (04-1130z), 24 April 92 (01-23z), 3 July 92 (01-23z), 20 July 92 (11-22z), 5 Oct 93 (07-18z), 8 Dec. 93 (10-18z) and 14 Dec. 93 (10-18z).

The thresholds and boundaries were produced essentially by applying the correlation technique to the aggregate tables. However, the correlation technique was modified for application to the 1-D tables because when the satellite classes assigned as rain in order of percentage of rain, they are not necessarily contiguous. The use of a threshold class or boundary implies that the classes assigned are contiguous. To obtain the 1-D thresholds, each class starting with class 32 (the coldest or brightest) was assigned as rain above the threshold rate and the total assigned compared with the number of pixels observed above that rate. The critical class was the last class assigned which gave the closest agreement with the number observed. The 1-D threshold is then either the visible count or infrared temperature at the lower boundary of the critical class or from the middle of the class. The middle of a class was used when one class boundary gave too few counts and the next one down too many.

Table 1 Infrared and Visible Thresholds

Threshold (mmh ⁻¹)	Infrared		Visible			
	CC	T(°C)	CC	Counts/2	Counts	Albedo
0.03	23	<-32	19+	>79	>158	>55%
0.125	24	<-34	20+	>81	>162	>56%
0.5	27	<-40	23	>86	>172	>60%
2.0	30	<-49	28+	>98	>196	>68%

Table 1 shows the 1-D thresholds. The + indicates that the threshold was taken as the middle of that class. The visible thresholds are expressed as Meteosat counts divided by 2, as used by FRONTIERS and the development software, and as Meteosat counts, as used by Nimrod. Equivalent values of albedo are also shown, calculated from the algorithm used by Autosat-2. This converts from raw Meteosat counts using an empirical calibration factor of $1.0 \text{ Wm}^{-2} \text{ sr}^{-1} \text{ count}^{-1}$ derived by Kriebal and Amman (1991). The thresholds for 0.03 mmh⁻¹ used in the current version of the Nimrod software are <-34°C and >162 visible counts. These were based on the work of Cheng et al. (1993), who produced thresholds for different synoptic types. It is very encouraging that the new data produce values so close to those obtained previously.

It is not so obvious how to assign contiguous classes within the 2-D tables. For example, one could build up a square or circular boundary. Therefore, the standard correlation was used ie the classes were assigned in order of percentage of rain. As expected, this meant that the boundary defined by the critical percentage enclosed some dry classes. Some classes were then redefined subjectively so that the boundary separated contiguous rain and no rain classes. This seemed justified on the grounds that the no rain "holes" often seemed due to small fluctuations in the percentage of rain. There was also a tendency to have no rain diagnosed in visible classes 15 and 16 in the colder infrared classes. Since there were few counts in these classes, the percentage of rain was subject to statistical uncertainty. Since there is no obvious reason why the brightest, coldest classes should not be associated with precipitation,

they were assigned as rain. This had a negligible impact on the number of rain counts assigned.

More adjustments were required as the threshold rate increased. In performing the adjustments the following factors were taken into consideration :-

- (i) the percentage of rain in the surrounding classes
- (ii) the shape of the boundary for the lower thresholds
- (iii) the effect on the total number of rain counts diagnosed, which should be kept to a minimum.

The following adjustments were made (classes given as IR,VIS) :-

0.03 mmh⁻¹

Change classes (13,16) to (16,16) to rain and class (7,14) to no rain, net increase 0.37% of the observed number.

0.125 mmh⁻¹

Change classes (13,16), (14,16), (16,16), (15,15) to rain, net increase 0.36%.

0.5 mmh⁻¹

Change classes (12,16) to (16,16), (12,15), (13,15), (15,15) (12,10) to rain and (10,10), (8,15) to no rain, net increase 4%.

2 mmh⁻¹

The classes assigned automatically were rather scattered so the boundary was calculated by hand starting from class (32,32). The boundary was designed to encompass as many of the classes assigned as rain automatically as possible, whilst following the shape of the boundary for the lower thresholds. The final boundary diagnosed the observed total number of rain counts to within + 1.3%.

Table 2 summarises the definition of the universal tables for all thresholds. The Ir/Vis. class numbers shown are those used in the Nimrod correlation scheme. The visible albedo and IR temperature at the lower boundary of each class are also shown. An interesting feature of Table 2 is the tendency to classify very cold but only moderately bright cloud as no rain. This is more pronounced than in the universal 2-D table produced from the work of Cheng et al. (1993). The most likely explanation for this feature is that it is associated with cold non-precipitating cirrus. One of the cases used to test the new scheme produced what appeared to be an unrealistically large area of precipitation over the north sea, associated with cold cirrus, when the FRONTIERS universal tables were used. This feature was assigned by the 2-D universal table because the satellite classes did not occur in the radar area. Use of the new universal table resulted in most of this feature being removed.

Table 2 Combined Definition of the 2-D Universal Tables

VIS/Alb.(%)	7	8	9	10	11	12	13	14	15	16
IR/T(°C)	48	51	54	57	60	63	65	69	78	88
7 (-12)										
8 (-16)			1	1	1	2	2	2	2	2
9 (-20)		1	2	2	3	3	3	3	3	3
10 (-25)		1	2	2	3	3	3	3	3	4
11 (-29)		1	2	2	3	3	3	4	4	4
12 (-33)			2	3	3	3	3	4	4	4
13 (-37)			2	3	3	3	4	4	4	4
14 (-41)			2	3	3	4	4	4	4	4
15 (-46)				2	3	4	4	4	4	4
16 (-55)							4	4	4	4

Key: 1 = $>0.03\text{mmh}^{-1}$
 2 = >0.03 and $>0.125\text{mmh}^{-1}$
 3 = >0.03 , >0.125 and $>0.5\text{mmh}^{-1}$
 4 = >0.03 , >0.125 , >0.5 and $>2\text{mmh}^{-1}$
 blank = no rain

4. Evaluation of Correlation Technique for All Thresholds

The ability of the correlation technique to delineate areas occupied by rain of intensity exceeding the thresholds has been evaluated by comparison with the FRONTIERS quality-controlled radar data within the FRONTIERS shallow layer UDB. This means that it is essentially the current correlation technique that is being evaluated because this is the first choice unless insufficient satellite counts are available in a class. This will be rare within the UDB when there is sufficient rain for evaluation. The same statistics are used as in previous studies ie the Critical Success Index (CSI), Probability of Detection (POD), False Alarm Ratio (FAR) and Tetrachoric Correlation Coefficient (TCC). CSI, POD and TCC have a value of 1 for perfectly correct forecasts and 0 for completely incorrect forecasts. FAR takes a value of 0 for perfectly correct forecasts and 1 for completely incorrect forecasts. CSI, POD and FAR have non-zero expectations (average score produced by random forecasts) and the average value of these is given as well. TCC has a zero expectation.

The cases and periods used are the same as used to construct the universal tables. The results are shown in Table 3.

Table 3 Average Statistics for Each Rainfall Rate Threshold**2-D**

Threshold	CSI	ECSI	POD	EPOD	FAR	EFAR	TCC
0.03	0.46	0.18	0.62	0.30	0.37	0.70	0.46
0.125	0.43	0.16	0.60	0.27	0.40	0.73	0.45
0.5	0.32	0.09	0.46	0.17	0.52	0.83	0.38
2.0	0.14	0.02	0.24	0.04	0.77	0.96	0.21

Visible

Threshold	CSI	ECSI	POD	EPOD	FAR	EFAR	TCC
0.03	0.38	0.19	0.55	0.32	0.46	0.70	0.34
0.125	0.34	0.16	0.50	0.27	0.50	0.73	0.32
0.5	0.23	0.09	0.38	0.18	0.64	0.84	0.24
2.0	0.07	0.02	0.17	0.06	0.86	0.96	0.10

Infrared

Threshold	CSI	ECSI	POD	EPOD	FAR	EFAR	TCC
0.03	0.37	0.18	0.53	0.30	0.47	0.70	0.33
0.125	0.34	0.15	0.49	0.25	0.50	0.74	0.32
0.5	0.24	0.09	0.38	0.16	0.62	0.84	0.27
2.0	0.10	0.02	0.20	0.05	0.84	0.96	0.14

It can be seen from Table 3 that the 2-D correlation table performs best for all thresholds. The visible and infrared correlation tables perform about the same for the low thresholds but infrared performs better for the 0.5 and 2 mmh⁻¹ thresholds. In earlier tests by Cheng et al. (1993) using only the 0.03 mmh⁻¹ threshold, visible scored better than infrared on average.

Table 4 CSI and TCC normalised to the value for a 0.03 mmh⁻¹ threshold

Threshold	2-D		Visible		Infrared	
	CSI	TCC	CSI	TCC	CSI	TCC
0.03	1.0	1.0	1.0	1.0	1.0	1.0
0.125	0.94	0.98	0.89	0.93	0.92	0.97
0.5	0.70	.82	0.60	0.71	0.66	0.80
2.0	0.30	0.45	0.19	0.30	0.27	0.42

The reduction in scores with increasing threshold rainfall rate is clarified by Table 4

where the CSI and TCC are normalised by the value for the lowest threshold. This shows that the performance of infrared alone only falls off marginally more than that of the 2-D technique. The performance of visible alone declines more quickly.

5. Variation of Average Rainfall Rate with Satellite Class

Figure 1 shows the average rainfall rate plotted as a function of satellite class for the visible and infrared data. Selected standard deviations are also shown. It can be seen from the slow variation of average rainfall rate with satellite class that there is only very limited rate information in the satellite data. This justifies the limited discrimination attempted in Nimrod and shows why attempts to diagnose 8 rainfall rate classes in early versions of FRONTIERS were unsuccessful.

The curves in Figure 1 are very similar to unpublished curves produced by P King, AES, Canada, using Goes satellite data. In particular, King also found the rapid increase in mean rate at high albedos, which does not occur at low IR temperatures. This may be due to the visible picking out intense convective cells at low solar elevations.

References

- Cheng, M, R. Brown and C. G. Collier, 1993. Delineation of precipitation areas using Meteosat infrared and visible data in the vicinity of the United Kingdom. *J. Appl. Met.*, 32, 884-898.
- Kriebal, K.T. and V. Amman, 1991. Absolute calibration of the Meteosat-4 VIS-channel. Proc. 8th Meteosat Scientific User's Meeting, Norrkoping, Sweden. EUM P 08, 33-38.
- Lovejoy, S. and G. L. Austin, 1979. The delineation of rain areas from visible and IR satellite data for GATE and mid-latitudes. *Atmos-Ocean*, 17, 77-92

FIGURE 1. AVERAGE RAINFALL RATE VS VISIBLE ALBEDO AND IR TEMPERATURE. SELECTED STANDARD DEVIATIONS ARE ALSO SHOWN.

